ISSN 0389-4010
UDC 533.6.011.8
519.245

NAL TR-1229T

TECHNICAL REPORT OF NATIONAL AEROSPACE LABORATORY

TR-1229T

Monte Carlo Simulation of Rarefied Nitrogen Gases Contained between Parallel Plates Using the Statistical Inelastic Cross-Section Model

Katsuhisa KOURA

March 1994

NATIONAL AEROSPACE LABORATORY

CHŌFU, TOKYO, JAPAN

Monte Carlo Simulation of Rarefied Nitrogen Gases Contained between Parallel Plates Using the Statistical Inelastic Cross-Section Model*

Katsuhisa KOURA*1

ABSTRACT

The statistical inelastic cross-section [SICS(D)] model for molecules with discrete rotational energy is used for the Monte Carlo simulation of rarefied nitrogen gases contained between two parallel plates at a large temperature difference with the null-collision direct-simulation Monte Carlo method to compare with the density distributions measured by Alofs et al. [Phys. Fluids **14**, 529 (1971)]. Good agreement is found between the experimental and Monte Carlo results for the fully diffuse reflection plates. The rotational distribution near the cold plate indicates the bimodal form represented approximately by the merging of two Boltzmann distributions at the cold and hot plate temperatures.

Key Words: Statistical inelastic cross-section model, Rarefied nitrogen gases between two parallel plates, Null-collision direct-simulation Monte Carlo method

概　　要

統計的非弾性衝突断面積 [SICS (D)] モデルを用いて，温度差の大きい二枚の平板間における希薄窒素分子の擬衝突直接シミュレーション・モンテカルロ法によるシミュレーションを行い，Alofs 等の密度分布測定結果と比較した。拡散反射壁に対するモンテカルロ結果は実験結果と良好な一致を示す。冷温壁近傍の回転分布は二つの壁温に対応するボルツマン分布の混合型を示す。

1. Introduction

In previous papers,[1,2] the statistical inelastic cross-section (SICS) model has been developed for the Monte Carlo simulation of molecules with discrete [SICS(D)][1] or continuous [SICS(C)][2] rotational energy and applied to the Monte Carlo simulation of nitrogen shock waves. It was shown that the SICS model reproduces well the measured rotational distributions as well as density and rotational temperature profiles through the shock wave.

In this paper, the SICS(D) model is used for the Monte Carlo simulation of rarefied nitrogen gases contained between two parallel plates at a large temperature difference with the null-collision direct-simulation Monte Carlo (NC-DSMC) method[1,3] in order to make a quantitative comparison with the density distributions measured by Alofs et al.[4] The rotational distribution, the translational and rotational temperatures, and the heat transfer between the plates are also obtained. Because the rotational distribution may be influenced by the mutual diffusion of molecules in various rotational levels, the variable soft sphere (VSS) molecular model[5] is employed for elastic molecular collisions.

In the Monte Carlo simulation the fully diffuse reflection plates may usually be assumed. However, by considering that the thermal accommodation coefficients determined from the free molecular heat-transfer measurements[4] with Knudsen's formula are not unity, the translational and rotational states of molecules reflected by the plate are taken such that a fraction α_t and α_r of the molecules impinging on

* Received May, 1993
*1 Aerodynamics Division

the plate emerges with the Maxwell and Boltzmann distributions at the plate temperature, respectively, while a fraction $(1-\alpha_t)$ and $(1-\alpha_r)$ of the molecules is specularly reflected. Because the translational (α_t) and rotational (α_r) reflection coefficients may be different from the measured thermal accommodation coefficient, the effects of the reflection coefficients are investigated.

2. Elastic and Inelastic Cross Sections

The cross section for elastic collisions is taken as the VSS model developed in Ref. 5 for both the viscosity and diffusion coefficients to be consistent with those of real gases. The differential elastic cross section $\sigma_{el}(\varepsilon, \chi)$ for the precollision relative energy ε and the deflection angle χ is given by

$$\sigma_{el}(\varepsilon, \chi) = \sigma_{el}(\varepsilon)\, P_{el}(\chi) \tag{1}$$

with the total elastic cross section

$$\sigma_{el}(\varepsilon) = c\varepsilon^{-\omega} \tag{2}$$

and the elastic probability density function of χ

$$P_{el}(\chi) = \alpha \cos^{2\alpha-1}(\chi/2) \sin(\chi/2). \tag{3}$$

The values of the VSS parameters, c, ω, and α, are listed in Ref. 5 for various gas species.

The cross section for rotationally inelastic collisions is taken as the SICS(D) model developed in Ref. 1 using the statistical assumption of the uncorrelation between the pre- and post-collision quantum states, the microscopic reversibility relation, and Parker's rotational energy gain function. The differential cross section $\sigma_{I',J'}(\varepsilon, \chi)$ for the rotational level transitions $I \rightarrow I'$ and $J \rightarrow J'$ is given by

$$\sigma_{I',J'}(\varepsilon, \chi) = \sigma_{I',J'}(\varepsilon)\, P_{rot}(\chi) \tag{4}$$

with the total rotational cross section

$$\sigma_{I',J'}(\varepsilon) = \zeta_{I'J'}(E)\, \sigma_{el}(\varepsilon) \tag{5}$$

and the rotational probability density function of χ

$$P_{rot}(\chi) = P_{el}(\chi). \tag{6}$$

The uncorrelation function $\zeta_{I'J'}(E)$ is given by

$$\begin{aligned} \zeta_{I'J'}(E) &= C(E) g_{I'} g_{J'} (E - E_{I'} - E_{J'}) \\ &\quad \times \sigma_{el}(E - E_{I'} - E_{J'}),\ E > E_{I'} + E_{J'}, \\ \zeta_{I'J'}(E) &= 0,\ E \le E_{I'} + E_{J'}. \end{aligned} \tag{7}$$

where $g_J = 2J+1$ and $E_J = k\theta_R J(J+1)$ are the degeneracy and energy of the Jth rotational level, respectively, k is the Boltzmann constant, θ_R is the characteristic rotational temperature, and $E = \varepsilon + E_I + E_J$ is the total energy. The function C(E) is given by

$$C(E) = 2\Delta E_R(E)/G_R(E) \tag{8}$$

with the rotational energy gain

$$\begin{aligned} G_R(E) = \{ & c/[2\,(2-\omega)(3-\omega)(4-\omega) \\ & \times (k\theta_R)^2] \}\, E^{4-\omega} \end{aligned} \tag{9}$$

for homonuclear diatomic molecules in even rotational levels and Parker's rotational energy gain function

$$\begin{aligned} \Delta E_R(E) = [& E/2 + (2\pi/3)(EE^*)^{1/2} \\ & + (\pi^2/4 + 2)E^*] / Z_R^{\infty}, \end{aligned} \tag{10}$$

where E^* is the potential well depth and Z_R^{∞} is the limiting value of Parker's rotational collision number.[6]

3. Monte Carlo Simulation

The Monte Carlo simulation of rarefied nitrogen molecules contained between two parallel plates maintained at the constant cold (T_c=79K) and hot (T_H=294K) temperatures is carried out using the NC-DSMC method[1,3] corresponding to the experimental conditions of Alofs et al.[4] The distance between the plates is taken to be L. The origin (x=0) of the position coordinate x perpendicular to the plates is taken at the center plane; the positions of the cold and hot plates are taken to be x=–L/2 and L/2, respectively. The computation domain between the plates is divided into small collision (data) cells with the same size of $\Delta x = L/100$. At initial time a large number of simulation molecules ($N=10^5$) are uniformly distributed between the plates with the equilibrium translational (Maxwell) and rotational (Boltzmann) distributions at the cold plate temperature T_c. The simulation procedures for molecular collisions described in Ref. 1 and for free molecular motions with collisions with the plates during a small time step Δt are separately repeated. The reflection coefficients α_t and α_r for the cold and hot plates are assumed to be identical. After the steady state is established, the physical quantities such as the rotational distribution y_J ($\Sigma_J y_J = 1$) and the rotational

temperature $T_r=\Sigma_j(E_j/k)y_j$ are calculated from accumulated molecular data.

The VSS parameters for nitrogen are taken to be those determined in Ref. 5 over the temperature range 100-300K corresponding to the plate temperatures T_c=79K and T_H=294K; i.e., ω=0.387 and c'=603 for $\sigma_{el}(\varepsilon)=c'(\varepsilon/k)^{-\omega}$ in Å^2 and ω_α=–0.0816 and c_α=2.595 for $\alpha=c_\alpha(\varepsilon/k)^{\omega\alpha}$. The SICS parameters for nitrogen are taken as those employed in Ref. 1; i.e., θ_R=2.878K, E*/k=91.5K, and Z_R^∞=21.

The experimental Knudsen number[4] $Kn_0=\lambda_0/L$ may be defined using the hard-sphere mean free path $\lambda_0=(\sqrt{2}n_0\sigma_0)^{-1}$ with the hard-sphere cross section σ_0 and the number density n_0 at the center plane. The value of σ_0 may be evaluated from the Knudsen number Kn_0 and the density $\rho_0=mn_0$ indicated[7] in Fig. 4 of Ref. 4, the molecular mass m, and the experimental plate distance[4] L=2.28 cm to be $\sigma_0=m(\sqrt{2}L\rho_0Kn_0)^{-1}$(~45.5Å^2). On the other hand, the center-plane number density n_0 cannot be evaluated a priori in the Monte Carlo simulation, where the mean free path is defined using the average number density <n> between the plates, and an iterative procedure is employed to obtain the value of Kn_0 close to the experimental one.

4. Results and Discussion

The number density n normalized by its center-plane value n_0 is compared in Figs.1-5 between the Monte Carlo results for $\alpha_t=\alpha_r$=1.0 (Kn_0=0.588, 0.293, 0.193, 0.111, and 0.054) and for $\alpha_t=\alpha_r$=0.82 (Kn_0=0.582, 0.290, 0.190, 0.110, and 0.054) and the experimental data[4] for Kn_0=0.583, 0.288, 0.191, 0.110, and 0.053, respectively, where the thermal accommodation coefficients were evaluated to be 0.82 from the free molecular heat-transfer measurements; the Monte Carlo values of Kn_0 obtained by

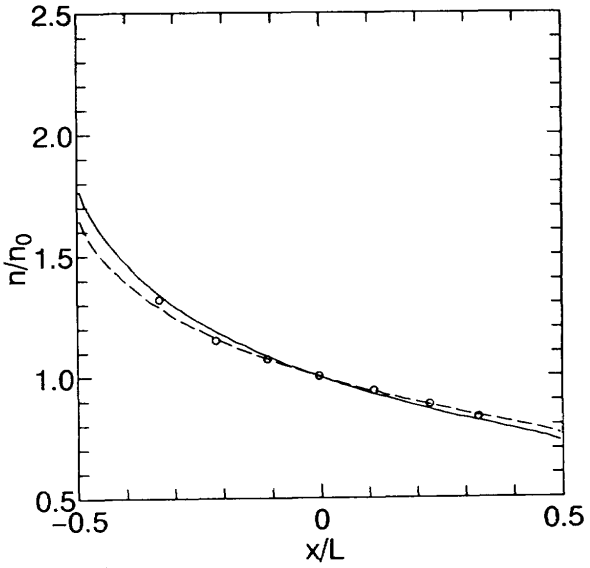

Fig. 2 Same as Fig. 1; Monte Carlo (— : $\alpha_t=\alpha_r$=1.0, Kn_0= 0.293; – – : $\alpha_t=\alpha_r$=0.82, Kn_0= 0.290); experimental (o : Ref. 4, Kn_0=0.288)

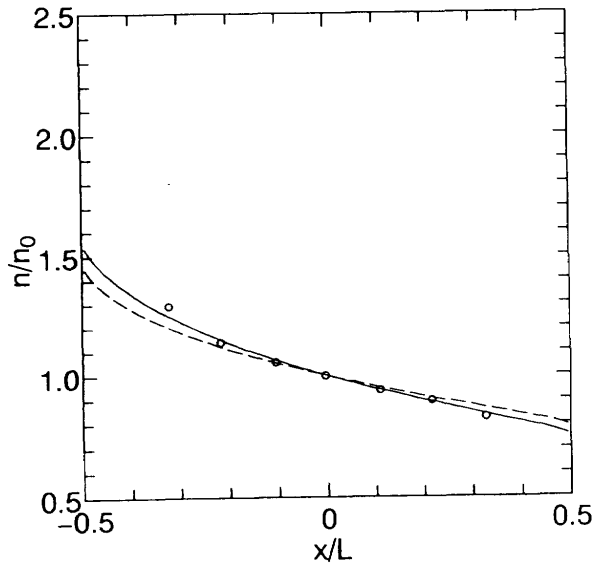

Fig. 1 Comparison of number density distribution between the Monte Carlo (— : $\alpha_t=\alpha_r$=1.0, Kn_0= 0.588; – – : $\alpha_t=\alpha_r$=0.82, Kn_0= 0.582) and experimental (o : Ref. 4, Kn_0=0.583) data

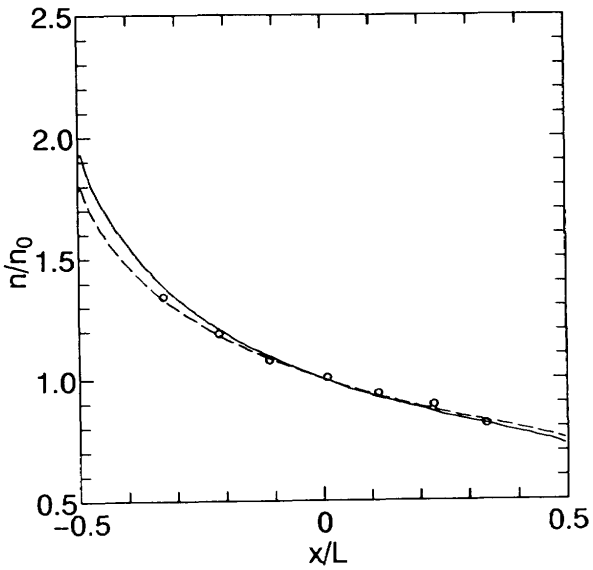

Fig. 3 Same as Fig. 1; Monte Carlo (— : $\alpha_t=\alpha_r$=1.0, Kn_0= 0.193; – – : $\alpha_t=\alpha_r$=0.82, Kn_0= 0.190); experimental (o : Ref. 4, Kn_0=0.191)

a single iteration agree with the experimental ones within 2%. The Monte Carlo results for $\alpha_t=\alpha_r=1.0$ and 0.82 agree well with the experimental data; for $Kn_0=0.583$ the Monte Carlo results for $\alpha_t=\alpha_r=1.0$ ($Kn_0=0.588$) are in better agreement with the measured data than for $\alpha_t=\alpha_r=0.82$ ($Kn_0=0.582$). The effects of the reflection coefficients on n/n_0 for $Kn_0=0.583$ are investigated over the range $0.5\leq \alpha_t, \alpha_r\leq 1.0$ but the best agreement is obtained for the fully diffuse reflection ($\alpha_t=\alpha_r=1.0$). The difference of the number density distribution between

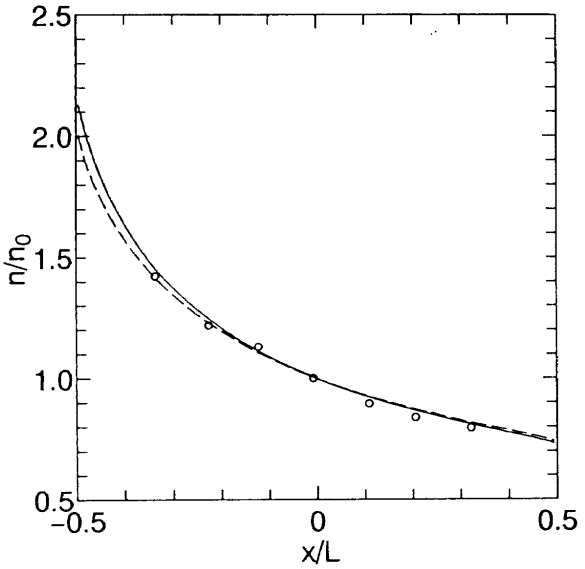

Fig. 4 Same as Fig. 1; Monte Carlo (— : $\alpha_t=\alpha_r=1.0$, $Kn_0=0.111$; – – : $\alpha_t=\alpha_r=0.82$, $Kn_0=0.110$); experimental (○ : Ref. 4, $Kn_0=0.110$)

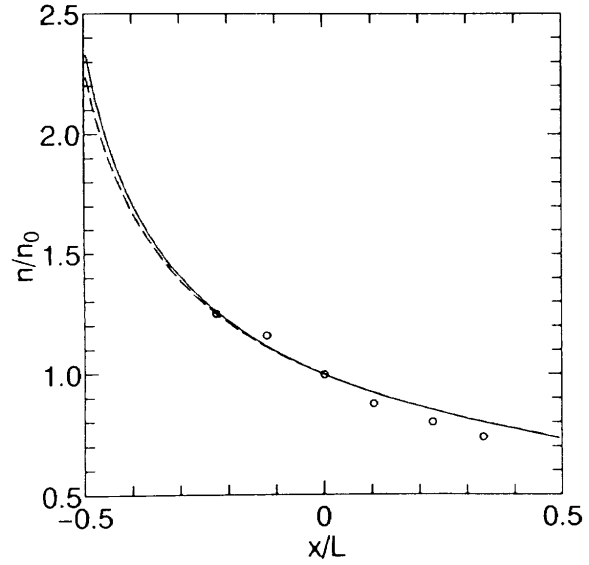

Fig. 5 Same as Fig. 1; Monte Carlo (— : $\alpha_t=\alpha_r=1.0$, $Kn_0=0.054$; – – : $\alpha_t=\alpha_r=0.82$, $Kn_0=0.054$); experimental (○ : Ref. 4, $Kn_0=0.053$)

$\alpha_t=\alpha_r=1.0$ and 0.82 decreases with the decrease in Kn_0 especially near the hot plate.

The translational (T) and rotational (T_r) tempera-tures normalized by the cold plate temperature T_c are shown in Figs. 6-10 for $\alpha_t=\alpha_r=1.0$ and 0.82 corresponding to the Knudsen numbers indicated for n/n_0 (Figs. 1-5). The discrepancy between the translational and rotational temperatures is larger near the hot plate than the cold plate and decreases

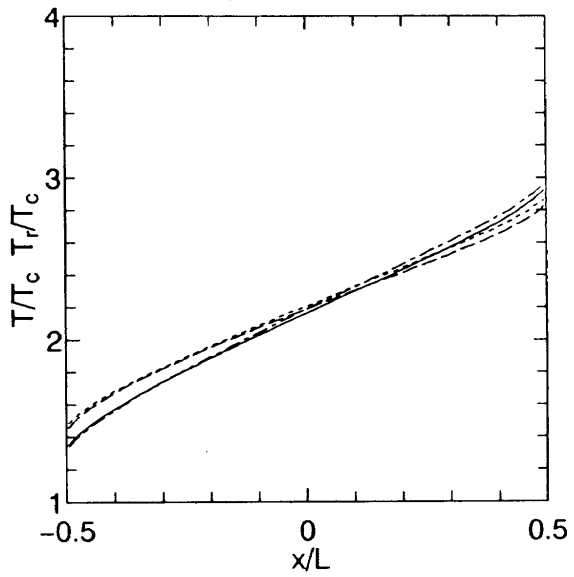

Fig. 6 Translational (— : $\alpha_t=\alpha_r=1.0$, $Kn_0=0.588$; – – : $\alpha_t=\alpha_r=0.82$, $Kn_0=0.582$) and rotational (– – – : $\alpha_t=\alpha_r=1.0$, $Kn_0=0.588$; ---- : $\alpha_t=\alpha_r=0.82$, $Kn_0=0.582$) temperature distributions

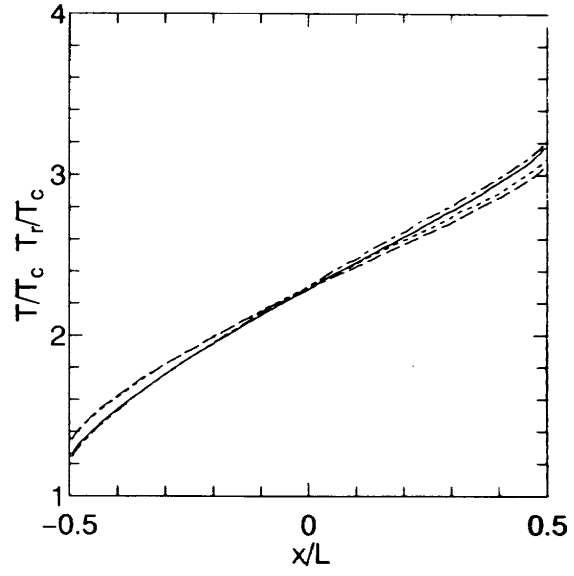

Fig. 7 Translational (— : $\alpha_t=\alpha_r=1.0$, $Kn_0=0.293$; – – : $\alpha_t=\alpha_r=0.82$, $Kn_0=0.290$) and rotational (– – – : $\alpha_t=\alpha_r=1.0$, $Kn_0=0.293$; ---- : $\alpha_t=\alpha_r=0.82$, $Kn_0=0.290$) temperature distributions

with the decrease in Kn_0. The difference of the temperature distributions between $\alpha_t=\alpha_r=1.0$ and 0.82 decreases with the decrease in Kn_0 especially near the cold plate.

The reduced rotational distribution y_J/g_J relative to that of the ground level (J=0) versus the rotational energy E_J in K is presented in Figs.11-15 for $\alpha_t=\alpha_r=1.0$ (Kn_0=0.588, 0.293, 0.193, 0.111, and 0.054); the difference of $\ln[(y_J/g_J)/(y_0/g_0)]$ between $\alpha_t=\alpha_r=1.0$ and 0.82 is small. It is noted that the rotational distribution near the cold plate indicates the bimodal form represented approximately by the merging of two Boltzmann distributions at the cold and hot plate temperatures; for the smallest Knudsen number Kn_0=0.054 the rotational distribution tends toward the local Boltzmann distribution.

In the Monte Carlo calculation, the total (trans-

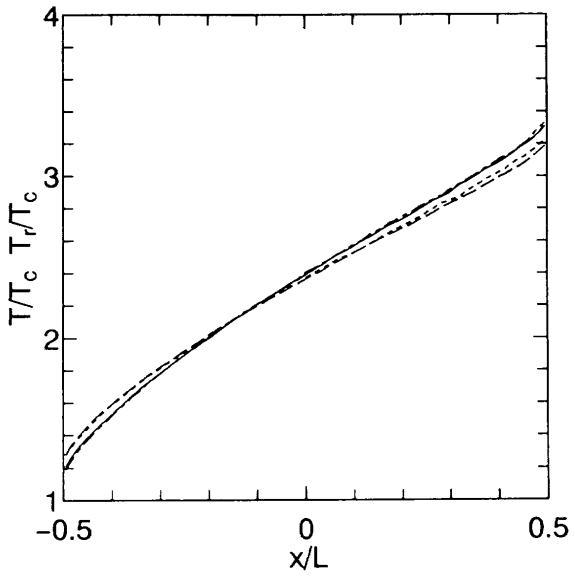

Fig. 8 Translational (— : $\alpha_t=\alpha_r=1.0, Kn_0=0.193$; – – : $\alpha_t=\alpha_r=0.82$, $Kn_0=0.190$) and rotational (– – – : $\alpha_t=\alpha_r=1.0, Kn_0=0.193$; ---- : $\alpha_t=\alpha_r=0.82, Kn_0=0.190$) temperature distributions

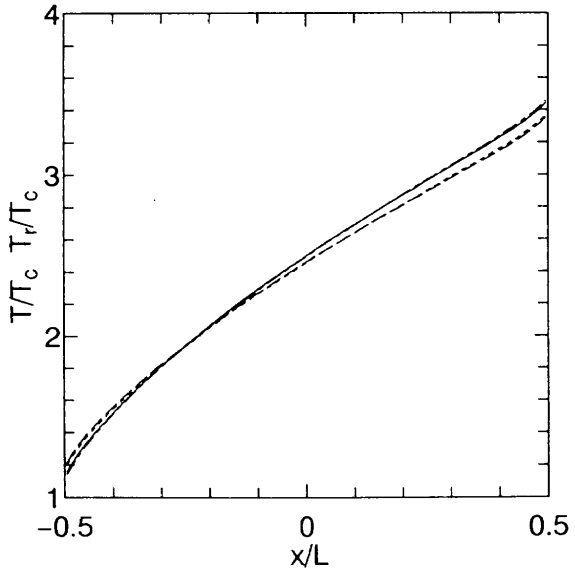

Fig. 9 Translational (— : $\alpha_t=\alpha_r=1.0, Kn_0=0.111$; – – : $\alpha_t=\alpha_r=0.82$, $Kn_0=0.110$) and rotational (– – – : $\alpha_t=\alpha_r=1.0, Kn_0=0.111$; ---- : $\alpha_t=\alpha_r=0.82, Kn_0=0.110$) temperature distributions

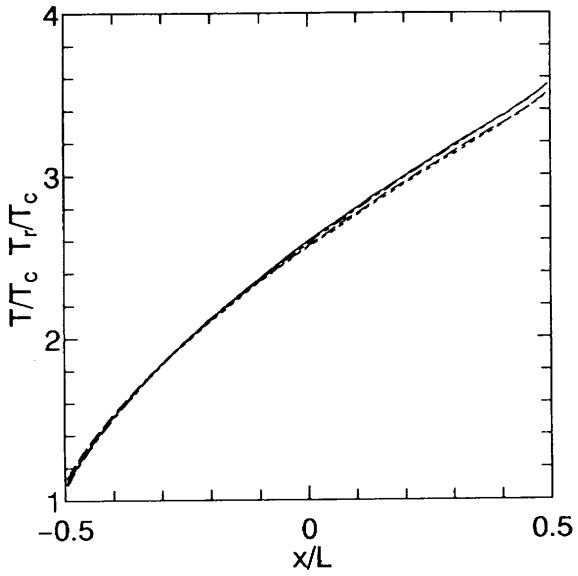

Fig. 10 Translational (— : $\alpha_t=\alpha_r=1.0, Kn_0=0.054$; – – : $\alpha_t=\alpha_r=0.82$, $Kn_0=0.054$) and rotational (– – – : $\alpha_t=\alpha_r=1.0, Kn_0=0.054$; ---- : $\alpha_t=\alpha_r=0.82, Kn_0=0.054$) temperature distributions

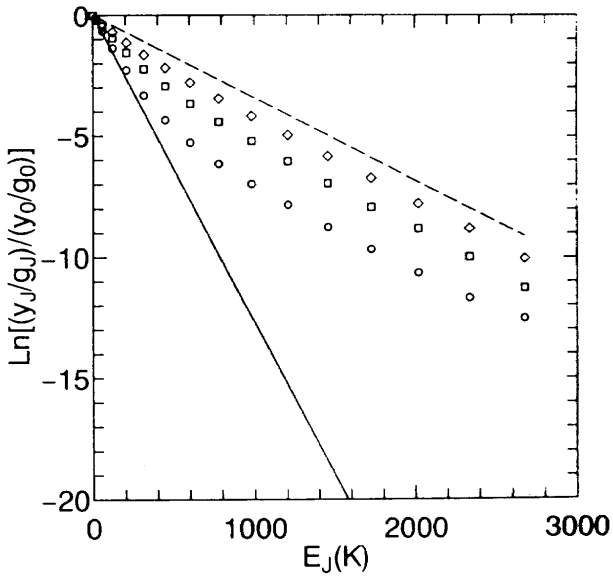

Fig. 11 Rotational distributions (○ : x/L=−0.495, □ : x/L=−0.005, ◇ : x/L=0.495) for $\alpha_t=\alpha_r=1.0$ and $Kn_0=0.588$ as compared with the Boltzmann distributions at the cold (—) and hot (– –) plate temperatures

lational and rotational) heat transfer Q is nondimensionalized by $< \rho > c^3/2$, where $< \rho >= m < n >$ is the average density between the plates and $c=(2kT_c/m)^{1/2}$ is the most probable speed at the cold plate temperature. The nondimensional free molecular value $Q_{fm}/(< \rho > c^3/2)$ is also obtained by the Monte Carlo simulation without molecular collisions. The total heat transfer normalized by its free molecular value, Q/Q_{fm} {$=[Q/(< \rho > c^3/2)]/[Q_{fm}/(< \rho > c^3/2)]$}, versus the inverse Knudsen number $1/Kn_0$ is presented in Fig. 16 for $\alpha_t=\alpha_r=1.0$ and 0.82 ($T_H/T_c=3.72$). It is confirmed that the values of $Q/(< \rho > c^3/2)$ or $Q_{fm}/(< \rho > c^3/2)$ for the cold and hot plates are coincident within 1%. Because there exist no experimental data at a large plate-temperature difference, the measured data[8] of Q/Q_{fm} at a very small plate-temperature difference ($T_H/T_c=1.03$), where the free molecular value Q_{fm} was evaluated from Knudsen's formula with the thermal accommodation coefficient of 0.76, and the Monte Carlo results obtained for $\alpha_t=\alpha_r=0.76$ and 0.60 at a small plate-temperature difference ($T_H/T_c=1.28$) are shown for comparison. The Monte Carlo values of Q/Q_{fm} increases with the decrease in the reflection coefficients. It is of interest to note that the Monte Carlo values for $\alpha_t=\alpha_r=0.76$ agree well with the measured

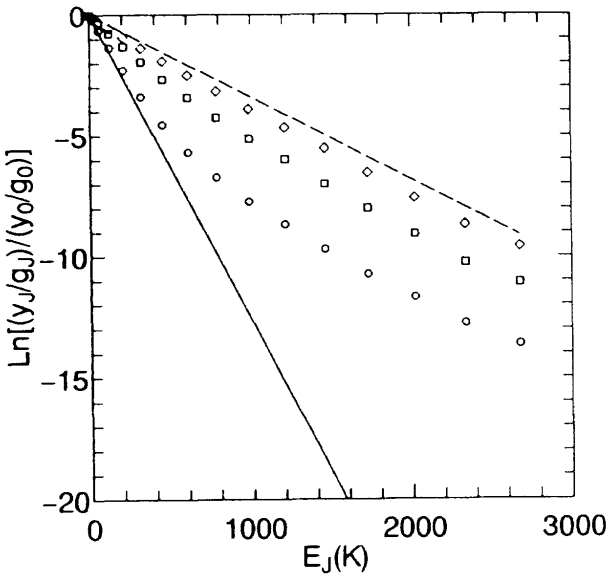

Fig. 12 Same as Fig. 11; $Kn_0=0.293$

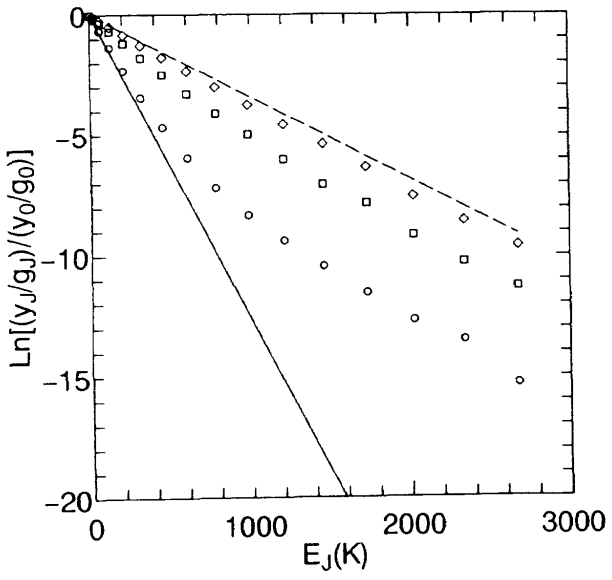

Fig. 13 Same as Fig. 11; $Kn_0=0.193$

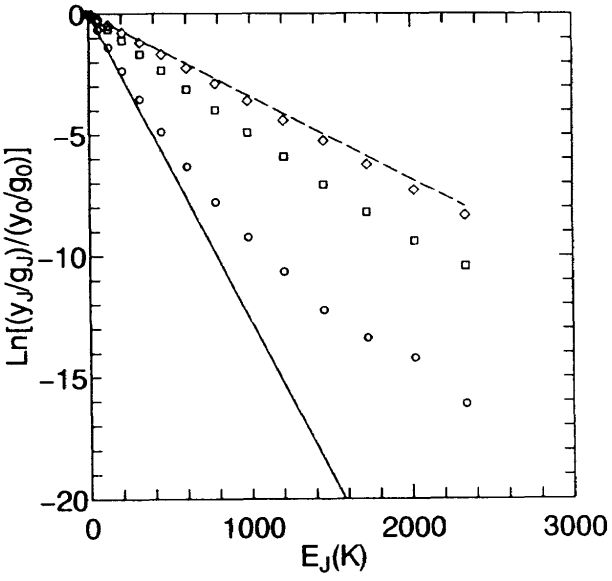

Fig. 14 Same as Fig. 11; $Kn_0=0.111$

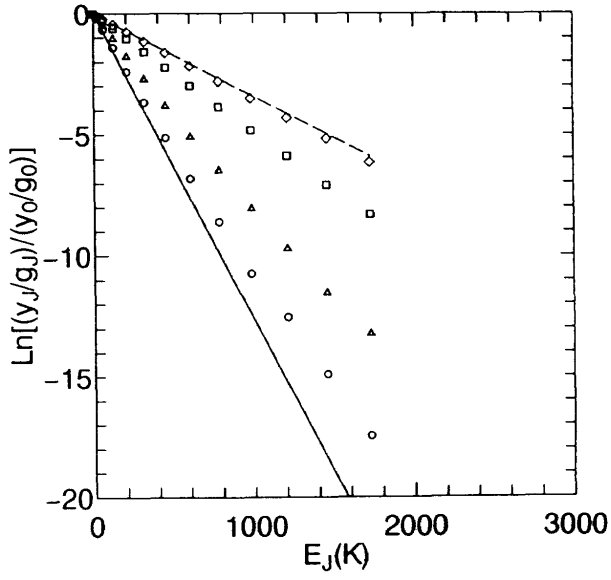

Fig. 15 Same as Fig. 11; △: x/L=−0.405; $Kn_0=0.054$

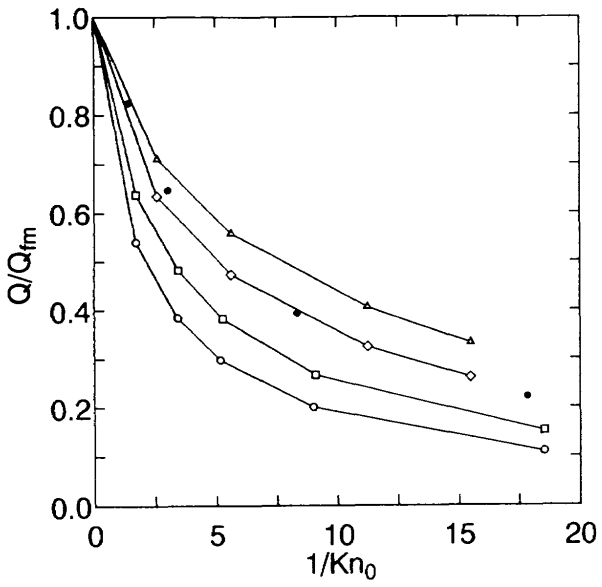

Fig. 16 Monte Carlo heat-transfer data (○ : $\alpha_t=\alpha_r=1.0$, □ : $\alpha_t=\alpha_r=0.82$; $T_H/T_c=3.72$) versus inverse Knudsen number as compared with the experimental (● : Ref. 8; $T_H/T_c=1.03$) and Monte Carlo (◇ : $\alpha_t=\alpha_r=0.76$, △ : $\alpha_t=\alpha_r=0.60$; $T_H/T_c=1.28$) data

data, although the definition of Q_{fm} as well as the reflection and accommodation coefficients and the plate temperatures are different.

5. Concluding Remarks

The SICS(D) model is used for the Monte Carlo simulation of rarefied nitrogen gases contained between two unequally heated parallel plates. It is found that the measured density distributions between the plates at a large temperature difference are well reproduced by the SICS(D) model for the fully diffuse reflection plates. The rotational distribution near the cold plate indicates the bimodal form represented approximately by the merging of two Boltzmann distributions at the cold and hot plate temperatures. It may be of interest to note that the bimodal pattern is similar to that observed in a hypersonic nitrogen shock wave.[9] It is hoped that a measurement of the rotational distribution between the plates at a large temperature difference will be made for the verification of the bimodal pattern.

References

1) K. Koura, "Statistical inelastic cross-section model for the Monte Carlo simulation of molecules with discrete internal energy," Phys. Fluids **A4**, 1782 (1992).

2) K. Koura, "Statistical inelastic cross-section model for the Monte Carlo simulation of molecules with continuous internal energy," Phys. Fluids **A5**, 778 (1993).

3) K. Koura, "Null-collision technique in the direct-simulation Monte Carlo Method," Phys. Fluids **29**, 3509 (1986); "Null collision Monte Carlo method: Gas mixtures with internal degrees of freedom and chemical reactions," Prog. Astronaut. Aeronaut. **117**, 25 (1989); "A sensitive test for accuracy in evaluation of molecular collision number in the direct-simulation Monte Carlo method," Phys. Fluids **A2**, 1287 (1990).

4) D.J. Alofs, R.C. Flagan, and G.S. Springer, "Density distribution measurements in rarefied gases contained between parallel plates at high temperature differences," Phys. Fluids **14**, 529 (1971).

5) K. Koura and H. Matsumoto, "Variable soft sphere molecular model for inverse-power-law or Lennard-Jones potential," Phys. Fluids **A3**, 2459 (1991); "Variable soft sphere molecular model for air species," Phys. Fluids **A4**, 1083 (1992); K. Koura, H. Matsumoto, and M. Takahira, "Variable soft sphere molecular model for the Monte Carlo simulation of air species," Prog. Astronaut. Aeronaut. (in press).

6) J.G. Parker, "Rotational and vibrational relaxation in diatomic gases," Phys. Fluids **2**, 449 (1959).

7) The units of the center-plane density ρ_0 given in Fig. 4 of Ref. 4 may read 10^{-8} g/cm^3 rather than 10^{-9} g/cm^3.

8) W.P. Teagan and G.S. Springer, "Heat-transfer and density-distribution measurements between parallel plates in the transition regime," Phys. Fluids **11**, 497 (1968).

9) F. Robben and L. Talbot, "Experimental study of the rotational distribution function of nitrogen in a shock wave," Phys. Fluids **9**, 653 (1966).

TECHNICAL REPORT OF NATIONAL
AEROSPACE LABORATORY
TR-1229T

航空宇宙技術研究所報告1229T号（欧文）

平成6年3月発行

発行所　航空宇宙技術研究所
東京都調布市深大寺東町7丁目44番地1
電話三鷹(0422)47-5911(大代表)〒182
印刷所　株式会社三興印刷
東京都新宿区西早稲田2-1-18

Published by
NATIONAL AEROSPACE LABORATORY
7-44-1 Jindaijihigashi-Machi, Chōfu, Tokyo
JAPAN

Printed in Japan